Optical properties of hair shafts estimated using the digital video microscopic system and inverse Monte Carlo method

Alexey N. Bashkatov[1*], Elina A. Genina[1], Andrey V. Volokh[1], Snezhana A. Murikhina[1], Gregory B. Altshuler[2], and Valery V. Tuchin[1]

[1]Saratov State University, Saratov, Russia, [2]Palomar Medical Products, Inc., Burlington, MA, USA

ABSTRACT

A color-camera-based technique was used for evaluation of reflectance and transmittance of the human hair shafts. The inverse Monte Carlo method was used for estimation of hair optical properties – absorption and reduced scattering coefficients. Hair samples have been obtained from ten volunteers. We have investigated blond, brown, black, light-brown and gray hairs. Obtained differences in absorption and scattering properties correlate with structure-morphological features of hair types. Offered method allows one to provide express-analysis of optical properties of a hair shaft, to determined separately absorption and scattering coefficients and melanin content.

Keywords: hair optical properties, digital image analysis, hair shaft, melanin, inverse Monte-Carlo method

1. INTRODUCTION

Knowledge of tissue optical properties is important for development of theoretical models describing the light propagation within tissues (including a human hair shaft). These models can be used when designing laser therapy and diagnostic techniques, or interpretation of spectrophotometric measurements. There are many papers describing the methods of determination of optical properties of many types of tissues.[1-12]

Objective quantitative estimation of optical properties of human hair shafts is necessary for study of morphology and pigmentation of a hair. This information is important for diagnostics and treatment of hair diseases, development of laser or lamp hair removal techniques.

There are a number of systems for such measurements.[1,8,12-14] Microspectrophotometry in wide-ranging of wavelengths is used for melanin concentration monitoring.[12] Low-coherent reflectometry is also a prospective method, which allows one to make measurements along and across a hair shaft with the high spatial resolution.[13] Unfortunately, these measuring systems are too sophisticated and expensive, therefore, could not be explored widely in clinical studies. In contrast, the digital analysis of images obtained with color video camera seems to be simple and cheap technique to obtain optical properties of a hair shaft or similar biological object.

The digital imaging method has been applied to evaluate the clinical morphology of different skin lesions (pigmentation, psoriasis, erythema, etc.), measurement of hair growth, wound healing, and burn management.[15-18]

In this study, we present technique for estimation of optical properties of hair shafts using the digital analysis of color images in both transmittance and reflectance modes and the inverse Monte Carlo code for evaluation of scattering and absorption coefficients.

2. OPTICAL PROPERTIES OF HUMAN HAIR SHAFTS

Absorption of hair is defined by the both concentration and type of melanin contained in the hair shafts (Fig. 1). Two types of melanin define full spectrum of colors of human hair: eumelanin, giving shades from brown to black, and pheomelanin, giving the yellow-blond, ginger, and red colors.[7,8,21,23] Absorption coefficient of melanin decreases with wavelength and it is rather small in NIR region.

[*] bash@optics.sgu.ru; Saratov State University, 155 Moskovskaya str., Saratov, Russia 410026.

Melanin is synthesized in melanocytes placed in the hair bulb on the top of the dermal papilla. Melanin is deposited in melanosomes. The actual color of hair depends on the sites and density of pigment deposition within the hair shaft and the shape of the pigment granules containing the pigment. Melanin granules are distributed throughout the hair cortex but in greater concentration toward the periphery.[23]

The pigment granules of black to brunette hair have an oval (rice grain) shape with a more or less homogenous inner structure and sharp boundaries; the surface is finely grained with a thin surrounding membrane-like layer of osmophilic material. Black hair granules are also relatively hard and have a high refractive index. Dark hairs shades have greater numbers of pigment granules per unit area than pale shades. Blonde and red hairs granules are more sparse, smaller, ellipsoid or spherical, and have a pitted surface.[23] Scattering properties of the hair shaft is defined by heterogeneity of its structure.

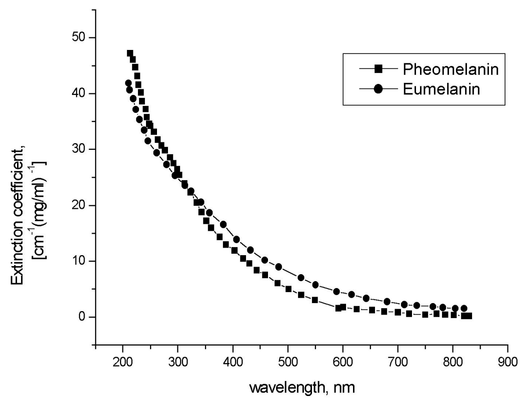

Fig. 1: Extinction coefficient spectra of melanins.[24]

White color of hairs is observed if the melanin is absent. It is caused by visual effect appeared due to the refraction and the reflection of light within the hair shaft. Thus, the nonpigmented hair shafts with a large medulla, as a rule, look lighter then the hair shafts without the medulla. The same effect is observed for worn and brittle hair shafts. In this case, the cortex and cuticle are noncontinuous. They form numerous surfaces with internal reflection and refraction of light. Consequently, such hair shafts look dark in transmission mode of light microscope. New formed nonpigmented hairs without the medulla look yellowish. Possibly this depends on the color of the dense keratin.[19,23]

The graying of hair is connected with the progressive degradation of melanocyte function and existence of large air spaces in the medulla of hair shafts, which cause strong scattering and internal reflection of light. In the graying hair gradual "dilution" of the pigment takes place, i.e. for individual hair shaft or from hair to hair various colors from natural to white can be observed. In a gray hair shaft melanocytes are found seldom, or are absent, or are inactive.[19]

Quantitative estimation of chromophores content in a scattering medium is based on the analysis of reflectance and/or transmittance spectra in the selected spectral range. Absorbance of a turbid medium $A(\lambda)$ is defined as $A(\lambda) = -\ln(R(\lambda))$ or $A(\lambda) = -\ln(T(\lambda))$, where $R(\lambda)$ is the reflectance at the wavelength λ and $T(\lambda)$ is the transmittance at the wavelength λ. These relations allow one to measure the relative changes of absorption properties of the scattering medium. Spectrum $A(\lambda)$ for melanin can be linear approximated in the spectral range from 620 to 720 *nm* and melanin content in tissue such as the human skin is determined as magnitude proportional to the linear slope of spectral dependence $A(\lambda)$ in this spectral range.[3,5,24]

The slopes of such linear approximations were used for estimation of melanin concentration in the human skin in the terms of DOPA melanin.[5] Using the absorbance measurements for DOPA melanin solutions of different concentrations the following linear approximation in the range 620-720 nm was received[5]

$$A = -\ln(T) = C_1 - C_2 \cdot 10^{-3} \cdot \lambda, \tag{1}$$

where A is the absorbance of DOPA melanin solution; T is the transmittance of DOPA melanin solution, λ is the wavelength in nm;

$$\begin{aligned} C_1 &= 0.0688 + 0.103 \cdot C, \\ C_2 &= 0.0794 + 0.124 \cdot C, \end{aligned} \tag{2}$$

C is the DOPA melanin concentration in mg/ml.

From the system of equations (2) we can obtain

$$C_1 = 0.84 \cdot C_2 \quad \text{and} \quad A(\lambda) = C_2(0.84 - \lambda \cdot 10^{-3}) = C_1(1 - \frac{\lambda \cdot 10^{-3}}{0.84}). \tag{3}$$

From (3) we can obtain:

$$\begin{aligned} C_1 &= \frac{A(\lambda)}{1 - \dfrac{\lambda \cdot 10^{-3}}{0.84}}, \\ C_2 &= \frac{A(\lambda)}{0.84 - \lambda \cdot 10^{-3}}. \end{aligned} \tag{4}$$

From the system of equations (2) we can obtain

$$C = \frac{C_1 - 0.0688}{0.103} = \frac{C_2 - 0.0794}{0.124}. \tag{5}$$

Thus, knowing the hair transmittance we can estimate the content of melanin in the hair shaft. The same method, but based on reflectance measurements was described for express estimation of melanin concentration.[1]

3. METHODS AND MATERIALS

For determination of optical parameters of a sample basing on spectrophotometric measurements the radiation transfer theory and any minimization procedure are usually used.[2,9,10,27] In this study the inverse Monte Carlo method was used for estimation of hair optical parameters from color images of hair shafts. Algorithm of statistical modeling is described in details in Ref. 25. The inverse algorithm is described in Ref. 26.

The scheme of the experimental setup is presented in Fig. 2. It provides *in vitro* digital analysis of images of biological objects in particular the human hair shafts. This technique allows one to estimate quantitatively transmittance and reflectance of a hair shaft in the specified spectral regions corresponding to three primary colors of the image (red, green, and blue).

The color imaging system is composed of a color video camera (SVHS Sony CCD-TR617E, PAL, Japan) and a light microscope interfaced with a personal computer. The examined object – a plane plate with attached biological object under study is illuminated by white light, which is guided to the object from the halogen lamp. Different modes of illumination provide either transmittance or reflectance images recording. In dependence on the mode of the illumination the plate presents either transparent subject glass (for the transmittance mode) or black & white test-object to provide the similar conditions of registration of images (for the reflectance mode). The size of illuminated place (10×10 mm) exceeds the field of vision of the system (1×1 мм). It assures the balancing illumination of the studied objects.

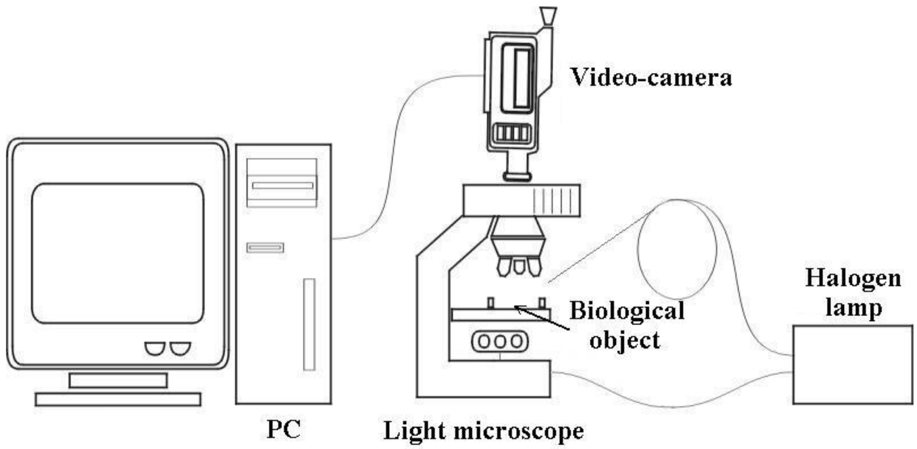

Fig. 2: Experimental setup for digital color analysis of biological objects.

The obtained image is processed by a personal computer as a standard BMP file. Such image is a set of data with a spatial resolution of 720 (horizontal) x 540 (vertical) pixels and a color resolution of 256 shades of the brightness for the each color band (red, green, and blue). The typical images of the light brown hair shaft in reflectance and transmittance modes are presented in Figs. 3 and 4, respectively.

To process the images of the hair shafts we have developed the special computer program with using Mathcad software (MathSoft Inc., USA). The base image was separated in three color matrixes of red, green, and blue components. The width of the scanning band along a hair shaft was 21 pixels (10 pixels up and down of the marker). Averaging of the measured values was done within this band. The choice of the scanning band was defined visually (glares, dust particles, particles of glue, and other external optical inhomogeneities were avoided). Furthermore, obtained curves were smoothed to remove the noise. As a result typical averaged scans of the hair shaft image for separated color components (red, green, and blue), corresponding to three spectral ranges for reflectance and transmittance measurements, are shown in Figs. 5 and 6. The brightness of images of the studied hair shaft and test-objects are expressed as shades of the brightness from 0 to 256.

To define reflectance of the hair shaft we took the ratio of the hair brightness (reflected intensity) I_h to the reference brightness (white paper) I_r for each color component. In addition, the background signal from black paper I_b was subtracted from both hair shaft brightness and reference brightness, respectively (see Fig. 3). Thus, the reflectance R was defined as

$$R = \frac{I_h - I_b}{I_r - I_b}, \tag{6}$$

where I_h, I_b, and I_r are the brightness (reflected intensity) of a hair shaft, background, and reference, respectively.

To define transmittance of a hair shaft we took the ratio of the hair brightness I_h to the reference brightness (the transparent glass) I_r for each color component (see Fig. 4). Thus, the transmittance T was defined as

$$T = \frac{I_h}{I_r}, \tag{7}$$

where I_h, and I_r are the brightness of a hair shaft and reference, respectively.

Fig. 3: Image of the human hair shaft (left) on the black & white test-object, recorded in reflectance mode (x 200).

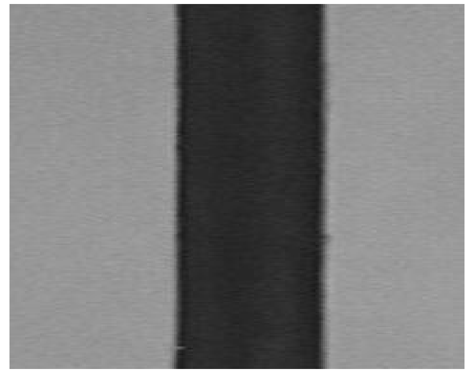

Fig. 4: Image of the human hair shaft on the subject glass, recorded in transmission mode (x 200).

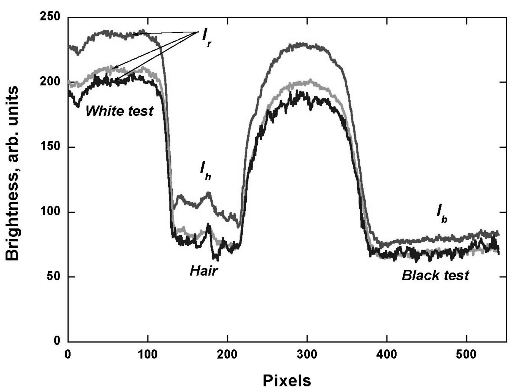

Fig. 5: The typical averaged scans of the hair shaft reflectance image for separated color components (red, green, and blue), corresponding to three spectral ranges. I_h, I_r, and I_b are the brightness of the studied hair shaft, white test-object (reference), and black test-object (background), respectively.

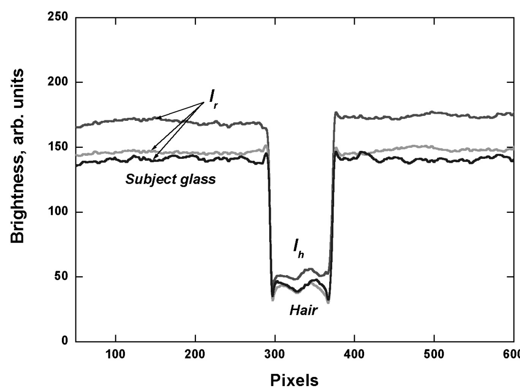

Fig. 6: The typical averaged scans of the hair transmittance image for separated color components (red, green, and blue), corresponding to three spectral ranges. I_h and I_r, are the brightness of the studied hair shaft and transparent glass (reference), respectively.

The estimation of wavelengths, and wavelength half-width of used color components was done in Ref 1: red - $\lambda_R = 600\,nm,\ \Delta\lambda_R = 51.4\,nm$, green - $\lambda_G = 540\,nm,\ \Delta\lambda_G = 74.1\,nm$, and blue - $\lambda_B = 460\,nm,\ \Delta\lambda_B = 47\,nm$.

4. RESULTS AND DISCUSSION

Samples of hair shafts were taken from 10 volunteers: I group – brown hair from woman, 19 yrs; II group – black hair from woman, 20 yrs; III group - graying fair hair from man, 45 yrs; IV group – blond hair from woman, 19 yrs; V group – gray hair from woman (earlier fair), 60 yrs; VI group – gray hair from woman (earlier brown), 70 yrs; VII – light brown hair from woman, 20 yrs; VIII - light brown hair from woman, 20 yrs; IX – gray hair from man (earlier fair), 70 yrs; X – light brown hair from man, 35 yrs. Each group includes 30 samples.

Absorption and reduced scattering coefficients were calculated for measured transmittance and reflectance using inverse Monte Carlo method – 1,000,000 photon packets with 10,000 photons in each packet were taken.

In Table 1 experimental values of diameter (micrometer measurements), transmittance and reflectance of hair shafts are presented. The data were averaged over 30 samples. It is seen that hair shafts of young people are thicker then of old ones. The dark hair shafts is thicker then fair hair shafts for the same age group. For all types of hair reflectance decreases and transmittance increases with the wavelength, i.e. scattering prevail absorption.

Table 1. Experimental data of digital processing of hair shafts images: *T* is the transmittance and *R* is the reflectance of hair shafts, respectively. Diameter was measured using mechanical micrometer.

Group	*Diameter* (μm*, mean* $\pm$ *sd*)	*Red component*		*Green component*		*Blue component*	
		T (mean ± sd)	*R* (mean ± sd)	*T* (mean ± sd)	*R* (mean ± sd)	*T* (mean ± sd)	*R* (mean ± sd)
I	57.6 ± 7.2	0.69 ± 0.18	0.014 ± 0.006	0.62 ± 0.18	0.025 ± 0.013	0.47 ± 0.12	0.030 ± 0.016
II	57.7 ± 4.8	0.63 ± 0.14	0.010 ± 0.005	0.55 ± 0.11	0.015 ± 0.010	0.38 ± 0.05	0.03 ± 0.03
III	48.2 ± 4.0	0.52 ± 0.07	0.09 ± 0.03	0.46 ± 0.06	0.11 ± 0.05	0.38 ± 0.05	0.14 ± 0.07
IV	39.9 ± 5.0	0.58 ± 0.09	0.08 ± 0.02	0.55 ± 0.08	0.08 ± 0.02	0.48 ± 0.07	0.10 ± 0.04
V	48.7 ± 5.8	0.47 ± 0.06	0.11 ± 0.02	0.45 ± 0.05	0.10 ± 0.02	0.40 ± 0.05	0.12 ± 0.03
VI	36.9 ± 2.6	0.58 ± 0.07	0.07 ± 0.02	0.52 ± 0.07	0.09 ± 0.03	0.47 ± 0.07	0.10 ± 0.04
VII	49.9 ± 5.2	0.67 ± 0.03	0.05 ± 0.02	0.61 ± 0.05	0.05 ± 0.03	0.50 ± 0.03	0.10 ± 0.08
VIII	60.2 ± 5.1	0.56 ± 0.07	0.07 ± 0.02	0.50 ± 0.06	0.09 ± 0.05	0.38 ± 0.04	0.11 ± 0.06
IX	41.6 ± 4.3	0.47 ± 0.07	0.11 ± 0.03	0.43 ± 0.07	0.11 ± 0.03	0.37 ± 0.05	0.14 ± 0.05
X	49.2 ± 4.1	0.62 ± 0.03	0.07 ± 0.03	0.54 ± 0.02	0.08 ± 0.04	0.43 ± 0.02	0.12 ± 0.09

Table 2 presents reconstructed values of absorption coefficient μ_a and reduced scattering coefficient μ'_s of the hair shafts for each spectral range.

Data of Table 2 illustrate that absorption coefficients of dark hair shafts (groups I and II) are high. They exceed absorption coefficients of many other tissues.[2,10]

It was noted that melanosomes are destructed and the output of melanin is discontinued at old age. Therefore, absorption coefficient of gray hair of old women with former brown hair color (group VI) is smaller then for young woman with brown hair (group I). Values of absorption coefficients of the light brown hair (groups VII, VIII, and X) are between values for brown-haired or brunette subjects and blond subjects. The absorption coefficient for young blond hairs (group IV) is comparable with the hair absorption coefficient for the old subjectss (groups V, VI, and IX) due to lack of melanin concentration. In the blond hair shafts melanin is absent. In the gray hair shafts melanin is destructed and could not be restored.

Spectral dependencies of the absorption coefficient of all hair groups are in a good accordance with the melanin spectrum (see Fig. 1). This correlation confirms the supposition that absorption properties of hair shafts are defined mostly by the natural pigment melanin.

Gray hair shafts show strong scattering. It is explained by their structure-morphological properties: rough surface, air-filled micro-cavities within a hair shaft, etc. The hair shafts of the both I group and II group (brown-haired subjects and brunettes) are weakly scattering. It is connected with the sizes of the scatterers, i.e. melanin granules. Light brown hair shafts take up mediate scattering properties between the dark and gray ones. It can be noted that blond and graying fair hair are similar due to some identity of their structure-morphological properties.

Table 2. Optical properties of the different hair types obtained using of inverse Monte Carlo method.

Group	*Red component* μ_a, (*1/cm*, mean ± sd)	*Red component* μ'_s, (*1/cm*, mean ± sd)	*Green component* μ_a, (*1/cm*, mean ± sd)	*Green component* μ'_s, (*1/cm*, mean ± sd)	*Blue component* μ_a, (*1/cm*, mean ± sd)	*Blue component* μ'_s, (*1/cm*, mean ± sd)
I	14.5 ± 3.8	40.6 ± 17.4	19.7 ± 5.7	55.8 ± 29.01	34.82 ± 8.90	90.5 ± 48.3
II	28.5 ± 6.3	37.5 ± 18.8	38.6 ± 7.7	53.4 ± 35.6	68.30 ± 8.99	91.3 ± 91.3
III	0.59 ± 0.08	164.5 ± 54.8	1.02 ± 0.13	202.6 ± 92.05	2.51 ± 0.40	278.2 ± 126.5
IV	0.45 ± 0.07	161.1 ± 40.3	0.78 ± 0.12	172.2 ± 42.5	1.93 ± 0.28	229.1 ± 91.6
V	0.77 ± 0.09	175.4 ± 31.8	1.32 ± 0.15	200.7 ± 40.2	3.27 ± 0.40	246.2 ± 63.7
VI	0.66 ± 0.09	182.5 ± 61.1	0.90 ± 0.13	209.4 ± 72.5	1.59 ± 0.25	257.5 ± 102.8
VII	2.05 ± 0.10	78.4 ± 26.5	2.77 ± 0.23	102.8 ± 61.2	4.89 ± 0.29	155.2 ± 124.0
VIII	3.35 ± 0.42	99.4 ± 28.4	4.54 ± 0.55	132.1 ± 80.9	8.02 ± 0.78	203.1 ± 110.7
IX	0.35 ± 0.05	233.6 ± 63.6	0.60 ± 0.10	268.3 ± 83.0	1.48 ± 0.20	331.4 ± 118.2
X	1.16 ± 0.06	105.9 ± 45.1	1.58 ± 0.06	142.3 ± 71.3	2.79 ± 0.13	223.2 ± 167.3

We have used the least-square approximation[26] to obtain the spectral dependences of the reduced scattering coefficient. Results are presented in Table 3. Reduced scattering coefficient in particular depends on the size[29] and number of the scatterers in the hair shafts. A numerator of the approximating expression characterizes the number of scatterers in the hair shaft.[10,11] It is seen that this number is large (about 10^9) for hair shafts of young subjects independently from hair type (dark or fair). For gray and blond hairs this number is much less, about 10^5. Wavelength exponent in denominator is determined mostly by sizes of the scatterers. Typically this parameter is in the range from 1 to 4; 1-2 corresponds to large Mie scatterers, and 4 – to small Rayleigh scatterers. Table 3 shows that exponent is about 3 for dark and fair hair of young subjects. This means that small scatterers predominate for these hair types. Melanin granules, keratin fibers, and fiber bundles are the scatterers in this case. In contrast, for gray and blond hair shafts the exponent is closed to 1. Therefore, as the predominant scatterers rather large scales on the surface and air-filled cavities within the medulla of the hair shafts can be considered.

Table 3. Spectral dependence of scattering properties of different hair types.

Group	*Approximation of the spectral dependence of reduced scattering coefficient*
I	$\mu_s' \approx 9.6 \cdot 10^9 / \lambda^3$
II	$\mu_s' \approx 8.2 \cdot 10^{10} / \lambda^{3.4}$
III	$\mu_s' \approx 5.1 \cdot 10^7 / \lambda^2$
IV	$\mu_s' \approx 7.4 \cdot 10^5 / \lambda^{1.3}$
V	$\mu_s' \approx 6.4 \cdot 10^5 / \lambda^{1.3}$
VI	$\mu_s' \approx 7.687 \cdot 10^5 / \lambda^{1.305}$
VII	$\mu_s' \approx 1.0 \cdot 10^9 / \lambda^{2.6}$
VIII	$\mu_s' \approx 3.1 \cdot 10^9 / \lambda^{2.7}$
IX	$\mu_s' \approx 1.1 \cdot 10^6 / \lambda^{1.3}$
X	$\mu_s' \approx 6.5 \cdot 10^9 / \lambda^{2.8}$

Estimation of the melanin content within the hair shaft was done in the number of studies.[1,12] Used method allows one to estimate the melanin content within the hair shaft from the transmittance or reflectance measurements. We have found the mean concentration of melanin in the different types of hairs using data for absorption coefficients (see Table 2) and for extinction coefficients of eumelanin and pheomelanin[24] (see Fig. 1). We assumed that for each hair type only one type of melanin (eumelanin or pheomelanin) is contained (see Table 4). Results are presented in Table 4. Comparison of presented data shows that use of the method of Ref. 1 leads to overestimation of the mean value of melanin concentration in the hair shaft in all groups.

Table 4. Melanin concentration in the hair shafts calculated using different methods.

Group	μ_a *(mg/ml, mean ± sd)*	*T (Ref. 1), (mg/ml, mean ± sd)*	*R (Ref. 1), (mg/ml, mean ± sd)*	*Type of melanin*
I	3.42 ± 0.43	12.44 ± 9.8	142.04 ± 17.8	Eumelanin
II	6.71 ± 1.02	14.98 ± 7.64	159.4 ± 18	Eumelanin
III	0.34 ± 0.09	21.62 ± 3.99	80.04 ± 10.01	Pheomelanin
IV	0.26 ± 0.08	18.43 ± 5.1	85.58 ± 9.2	Pheomelanin
V	0.44 ± 0.11	23.1 ± 4.93	77.58 ± 7.64	Pheomelanin
VI	0.16 ± 0.03	19.16 ± 4.5	83.91 ± 14.6	Eumelanin
VII	0.48 ± 0.08	13.2 ± 1.78	102.52 ± 12.4	Eumelanin
VIII	0.79 ± 0.2	18.43 ± 4.1	91.18 ± 33.3	Eumelanin
IX	0.2 ± 0.04	25.21 ± 5.08	73.72 ± 11.3	Pheomelanin
X	0.27 ± 0.02	15.96 ± 1.81	92.21 ± 17.33	Eumelanin

The reason of such differences is clear. In the both cases (as at the analysis of the image recorded in transmission mode as at the analysis of the image recorded in reflection mode), the both absorption and scattering properties of the hair shaft have not been separated. At the assignment of the full optical density of the hair shaft to the absorption of light by melanin, the high conservation of the mean values of melanin concentration in the hair shaft takes place.

Thus, the best result at the analysis of the optical properties of hair shafts can be obtained if the separation of the absorption and the scattering properties with using of the inverse Monte Carlo method is realized.

5. CONCLUSION

Hair shafts optical properties were studied using color digital imaging and inverse Monte Carlo method. The grounds of this method was considered and experimental setup allowing one to estimate transmittance and reflectance of a hair shaft for three spectral regions were presented. The inverse Monte Carlo method has allowed us to separate scattering and absorption properties of a hair shaft. Approximating expressions for the wavelength dependence of scattering coefficients for different types of hairs are found. Such expressions are is in a good accordance with structure-morphological properties of hair types. Analysis of the absorption properties of the hair shafts has allowed revealing shortcomings of methods of estimation of melanin content in hair shafts suggested earlier.

ACKNOWLEDGEMENT

The research was done due to financial support of grant "Leading Scientific Schools" No. 00-15-96667 of the Russian Basic Research Foundation and by Award No. REC-006 of the U.S. Civilian Research & Development Foundation for the Independent States of the Former Soviet Union (CRDF).

REFERENCES

1. A.N. Bashkatov, Yu.P. Sinichkin, E.A. Genina, et al., "RGB video microscopic system for *in vitro* monitoring of optical properties of hair shaft and follicle," *Proc.* SPIE, **4244**, pp. 161-167, 2001.
2. W.-F. Cheong, S.A. Prahl, A.J. Welch, "A review of the optical properties of biological tissue," IEEE *J. Quantum Electr.* **26** (12), pp. 2166-2185, 1990.

3. J.B. Dawson, D.J. Barker, D.J. Ellis, et al., "A theoretical and experimental study of light absorption and scattering by *in vivo* skin," *Phys. Med. Biol.* **25** (4), pp. 695-709, 1980.
4. N. Kollias and A. Baqer, "Spectroscopic characteristics of human melanin in vivo," *J. Investig. Dermatol.* **85**, pp. 38-42.
5. N. Kollias and A. Baqer, "On the assessment of melanin in human skin in vivo," *Photochem. and Photobiol.* **43** (1), pp. 49-54, 1986.
6. N. Kollias, R.M. Sayer, L. Zeise, et. al., "Photoprotection by melanin," *J. Photochem. Photobiol. B.* **9**, pp. 135-160, 1991.
7. I.A. Menon, S. Persad, H.F. Haberman, and C.J. Kurian, "A comparative study of the physical and chemical properties of melanins isolated from human black and red hair," *J. Investig. Dermatol.* **80** (3), pp. 202-206, 1983.
8. E.M. Nicholls, "Microspectrophotometry in the study of red hair," *Ann. Hum. Genet. Lond.* **32** (15), pp. 15-26, 1968.
9. S.A. Prahl, *Light transport in tissue*, Ph.D. dissertation, Univ. Texas at Austin, 1988.
10. V.V. Tuchin, *Tissue optics: Light Scattering Methods and Instruments for Medical Diagnosis,* SPIE Press, TT38, Bellingham, USA, 2000.
11. M.J.C. van Gemert, S.L. Jacques, H.J.C.M. Sterenborg, and W.M. Star, "Skin optics," IEEE *Transactions on Biomed. Ing.* **36** (12), pp. 1146-1154, 1989.
12. D.A. Zimnyakov, G.V. Simonenko, A.N. Bashkatov, et al., "Spatial-resolved microspectrophotometry for hair optical properties and geometry studies: CCD hair tester," *Proc.* SPIE **4244**, pp. 156-160, 2001.
13. X.J. Wang, N.E. Milner, R.P. Dhond, et al., "Characterization of human scalp hairs by optical low-coherence reflectometry," *Opt. Lett.* **20**, pp. 524-526, 1995.
14. N.V. Joshi, and J. Goyo-Rivas, "Optical and morphological investigation of hair of patients of Chediak Higashi syndrome," *Proc.* SPIE **3251**, pp. 229-234, 1998.
15. H. Takiwaki, S. Shirai, Y. Kanno, Y. Watanabe, and S. Arase, "Quantification of erythema and pigmentation using a videomicroscope and a computer," *Br. J. Dermatol.* **131**, pp. 35-92, 1994.
16. R.D. Kenet, "Digital imaging in dermatology," *Clinics in Dermatol.* **13**, pp. 381-391, 1995.
17. J. Steinmetz, and P. Bjerring "Video-optical monitoring of wheal and flare reactions. Effects of topical Na-sucrose-sulphate," *Skin Res. Technol.* **1**, pp. 90-95, 1995.
18. R. Marchesini, S. Tomatis, C. Bartoli, et al., "*In vivo* spectrophotometric evaluation of neoplastic and nonneoplastic skin pigmented lesions-III. CCD camera-based reflectance imaging," *Photochem. Photobiol.* **62**, pp. 151-154, 1995.
19. A. Rook, and R.P.R. Dawber, *Diseases of the Hair and Scalp*, Blackwell Scientific Publications, Oxford, London, Edinburgh, Boston Melbourne, 1984.
20. A.P. Bertolino, L.M. Klein, and I.M. Freedberg, "Biology of hair follicles," in *Biology and Function of Epidermis and Appendages* pp. 289-293.
21. E.J. Van Scott, T.M. Ekel, and R. Auterback, "Determinants of rate and kinetics of cell division in scalp hair," *J. Investig. Dermatol.* **41**, p. 269, 1963.
22. Y.S. Ryabukhin, "International coordinated program of trace element pollutans in human hair," in *Hair. Trace Elements and Human Illnesses,* eds. A.C. Brown, R.G. Crounse. New York, Praeger, Ch. 1, 1980, p. 5.
23. R.P.R. Dawber, *Hair color in Physical Properties of Hair,* CRC Press Inc., 1995, pp. 531-534.
24. S. Jacques, Published on the personal web-site: www.omlc.ogi.edu
25. I.V. Yaroslavsky and V.V. Tuchin, "Light propagation in multilayer scattering media: modeling by the Monte Carlo method," *Opt. Spectrosc.* **72**, pp. 505-509, 1992.
26. W.H., Press, S.A. Tuekolsky, W.T. Vettering, B.P. Flannery, *Numerical Recipes in C: The Art of Scientific Computing*, Cambridge: Cambridge University Press, 1992.
27. S.R. Arridge, "The forward and inverse problems in time resolved infra-red imaging," in SPIE. *Medical Optical Tomography: Functional Imaging and Monitoring* pp. 35-64, 1993.
28. I.V. Yaroslavsky, A.N. Yaroslavsky, T. Goldbach, et al., "Inverse hybrid technique for determining the optical properties of turbid media from integrating-sphere measurements," *Appl. Opt.* **35**, (34), pp. 6797-6809, 1996.
29. C.F. Bohren and D.R. Huffman, *Absorption and Scattering of Light by Small Particles*, Willey, New York, 1983.